



HAL
open science

Growth of a single bubble in semi-hard cheese: comparison between simulation and experiment

Yannick Laridon, David Grenier, Christophe C. Doursat, Delphine
Huc-Mathis, Nathalie Roland, D. Flick, Tiphaine Lucas

► **To cite this version:**

Yannick Laridon, David Grenier, Christophe C. Doursat, Delphine Huc-Mathis, Nathalie Roland, et al.. Growth of a single bubble in semi-hard cheese: comparison between simulation and experiment. Food Research International, 2020, 129, pp.9. 10.1016/j.foodres.2019.108858 . hal-02609862

HAL Id: hal-02609862

<https://hal.inrae.fr/hal-02609862>

Submitted on 12 May 2022

HAL is a multi-disciplinary open access archive for the deposit and dissemination of scientific research documents, whether they are published or not. The documents may come from teaching and research institutions in France or abroad, or from public or private research centers.

L'archive ouverte pluridisciplinaire **HAL**, est destinée au dépôt et à la diffusion de documents scientifiques de niveau recherche, publiés ou non, émanant des établissements d'enseignement et de recherche français ou étrangers, des laboratoires publics ou privés.



Growth of a single bubble in semi-hard cheese: Comparison between simulation and experiment



Y. Laridon^{a,*}, D. Grenier^a, C. Doursat^b, D. Huc^a, N. Roland^c, D. Flick^b, T. Lucas^a

^a Irstea, 17 Avenue de Cucillé, CS 64427, 35044 Rennes Cedex, France

^b UMR Ingénierie Procédés Aliments, AgroParisTech, INRA, Université Paris-Saclay, Massy, France

^c Laboratoires Standa, 68 Rue Robert Kaskoreff, Caen 14000, France

ARTICLE INFO

Keywords:

Multiphysics modelling
Mass transport
Momentum transport
Sensitivity analysis
Eye
Ripening

ABSTRACT

This paper proposes a model for bubble growth in semi-hard cheese coupling mechanical behaviour and mass transport. The modelling follows previous work centred on the mechanical aspects, and focuses in this paper on the mass transport phenomena. Data are compared to experimental results obtained on industrial-size cheeses, both under the rind and at core, and a sensitivity study is conducted to discuss the results. The model is in agreement with experiment at core, and underlines the great influence of the carbon dioxide production rate and the amount of cheese material surrounding the bubble on bubble growth. Under the rind, the model yielded poorer agreement, due to the fact that this region in the cheese is less homogeneous, and therefore with more intra- and inter-batch variation on the parameters that were characterized.

1. Introduction

Whilst bubbles are found in numerous food products (Campbell & Mougéot, 1999), the modelling of bubble growth for foodstuffs was almost exclusively limited to the study of sparkling beverages or cereal products. The studies on the former are inspired by nucleation studies in liquids, while for the latter, the studies are inspired by the works on polymer foaming (e.g. the works of Amon & Denson, 1984). The dynamics involved for the growth of bubbles in cheese encourages considering the present study as a continuation of works on bread dough proving. In the following, the state of the art in the modelling of dough proving is presented, with its similarities and its limitations for application to the case of cheese ripening. The availability in the literature of values for the input parameters required for this modelling task is discussed for the cheese material and semi-hard cheese in particular.

Bubbles nucleation in aerated products usually requires two conditions: a supersaturated environment and a catalytic site (Bisperink & Prins, 1994). For weakly supersaturated products such as sparkling beverages, nucleation requires a catalytic site, either a pre-existing gas pocket (usually imperfection on the glass-wall) or the presence of an alien substance (Jones, Evans, & Galvin, 1999; Liger-Belair, Parmentier, & Jeandet, 2006). For semi-hard cheeses, the cheese material is indeed supersaturated with carbon dioxide, though only slightly, and the catalytic site consists of gas pockets existing between curd grains (Akerman, Walstra, & Dijk, 1989; Huc, Mariette, et al., 2014). The

complexity of bubble nucleation makes it a subject of its own and exceeds the scope of the present study, which focuses on the next stage, the bubble growth.

Few modelling studies on aerated cereal products went to the extent of characterising the growth in cereal products at the bubble scale (De Cindio & Correra, 1995; Fan, Mitchell, & Blanshard, 1999; Hailemariam, Okos, & Campanella, 2007; Shah, Campbell, McKee, & Rielly, 1998), this selection encompassing both modelling studies on proving (De Cindio & Correra, 1995; Shah et al., 1998) and baking. The dough is often thought of as a purely viscous material, but some studies considered viscoelastic models. De Cindio and Correra (1995) considered the dough with a linear viscoelastic model very similar to that used in the present study. They showed that, contrary to the viscous models, the use of viscoelastic constitutive equations allowed to reproduce cases that had asymptotic bubble volumes due to the time-independent elastic properties of their viscoelastic modelling. Some other studies considered non-linear viscoelastic models, such as the Lodge model used by Hailemariam et al. (2007), that give a better description of the material behaviour, but necessitate a more time-consuming evaluation of the input parameters (the Lodge model enforces the knowledge of memory function for the material). They found that viscoelasticity of the dough tends to prevent bubbles from collapsing.

Mass transfer was proved to be the main contributing factor to bubble growth during dough proving (De Cindio & Correra, 1995;

* Corresponding author.

E-mail address: yannick.laridon@gmail.com (Y. Laridon).

<https://doi.org/10.1016/j.foodres.2019.108858>

Received 21 August 2019; Received in revised form 20 November 2019; Accepted 20 November 2019

Available online 02 December 2019

0963-9969/ © 2019 Elsevier Ltd. All rights reserved.

Hailemariam et al., 2007). Mass transport in the liquid phase can be modelled by Fick's law and applied to the liquid water in the case of dough proving; it should be extended to both the liquid water and liquid fat in the case of cheese (Jakobsen, Jensen, & Risbo, 2009). Exchanges at the bubble-material interface are often described using Henry's law. Shah et al. (1998) discussed the influence of the carbon dioxide saturation on the bubble growth, and showed that for sub-saturation regime, bubbles were to have an asymptotic size, that was influenced mainly by the initial bubble size and carbon dioxide concentration. For supersaturation regime, they showed that above a critical size, bubble growth would continue indefinitely. No asymptotic bubble size could be observed in the type of cheese studied in the present paper (Huc, Mariette, et al., 2014), evidencing that supersaturation also happens in the semi-hard cheese under study.

Despite the similarity of the driving phenomena between bread dough proving and cheese ripening, some differences have to be underlined. The rate of dough proving in bread manufacture is substantially faster (several hours) than eye formation in semi-hard cheese (several weeks). This discrepancy in the kinetics may be explained by differences in the microbiological phenomena involved. Carbon dioxide production in semi-hard cheese is caused by propionic fermentation, whereas it is caused by alcoholic fermentation for bread dough, and the optimal conditions of carbon dioxide production, in terms of temperature or pH for instance, highly differ between the two processes. The bubble growth kinetics may also be influenced by the mechanical behaviour of the material surrounding the bubbles. Although both materials (dough and cheese) are viscoelastic materials with similar relaxation time spectrum (Keentok, Newberry, Gras, Bekes, & Tanner, 2002), viscoelasticity of cheese is one to two orders of magnitude higher than that of bread doughs (Launay & Michon, 2008). Compared to about 10% for semi-hard cheeses at the end of ripening (Huc, Mariette, et al., 2014), bread dough is a highly porous product: if its porosity is of 20% at the end of mixing, it increases up to 70–90% at the end of baking. The bubbles in cheese are also typically a couple of centimetres in size at the end of ripening, larger than those in bread dough which are typically only a couple of millimetres in size, and for which surface tension effects are not negligible.

Experimental validation of the models focused on dough proving and baking, when implemented, often took place at a macroscopic level, by using overall morphologic descriptors (Chiotellis and Campbell, 2003; Fan et al., 1999). Both characteristic size of bubble and their rate of growth in cheese are compatible with tomographic monitoring, hence offering for the first time the possibility to validate the modelling of bubble growth in food material at the scale of the bubble.

For appropriate validation, the model of transport has also to be fed with values for several input parameters, specific for mass transport and production and appropriate for semi-hard cheeses, such as carbon dioxide diffusivity, solubility and production rate. There are very few papers dedicated to the estimation of carbon dioxide diffusivity in semi-hard cheese. The notable exception is the study from Acerbi, Guillard, Guillaume, Saubanere, et al. (2016), conducted on the same type of semi-hard cheese as in the present paper, measured at various pH, salt content, moisture or cheese age. Numerous studies, however, were carried out on cheese in modified atmosphere packaging, and focused on the exchange of carbon dioxide at the product interface. These studies provide data on interfacial transfers for a wide variety of products, for instance the work on Swiss-type cheese by Blanc, Bosset, Martin, and Jimeno (1983); however, they fail to disentangle the respective influence of diffusion and production within the product by focusing on the interface only. Rodriguez-Aguilera, Oliveira, Montanez, and Mahajan (2009) and Vivier, Compan, Moulin, and Galzy (1996) successfully estimated carbon dioxide production rate, but their study was applied to soft cheeses, for which the fermentation mechanism differs from that of semi-hard cheeses. In semi-hard cheeses, the carbon dioxide production originates from propionic fermentation, but also from proteolysis (to a lesser extent, only 20%, ITFF-ITG/Actilait, 1984).

Some studies were conducted to investigate the influence of several manufacturing parameters on bubble growth in cheese (Guggisberg et al., 2015; Schuetz et al., 2013), and while they successfully used non-invasive tomographic measures to discuss the effects of these parameters on the bubble volume or aspect, their approach remained empirical and did not provide a mechanistic model. Finally, some studies have estimated the carbon dioxide solubility in cheese, but on the whole cheese block, and only at the end of the ripening (Jakobsen et al., 2009; Seuvre & Mathlouthi, 1982).

The purpose of the present paper was to implement a model of the coupled mechanical behaviour and mass transport in the case of a single bubble growth in semi-hard cheese. The study also aimed at identifying input parameters of the model that were the most influential on bubble growth; this part of the study was based on a compilation of literature data for input parameters but also on the measurement of some specific ones, such as carbon dioxide production rate, concentration of CO₂ in cheese at saturation and mechanical properties of the cheese material. At last, the study aimed at comparing the simulations of this model to experimental data. The bubble growth was monitored by MRI (Magnetic Resonance Imaging) and X-Ray Imaging on industrial cheese blocks during ripening (warm room). The mechanics involved in the bubble growth were already validated on a separate experiment involving known pressure forces (Y. Laridon et al., 2016), allowing the focus of the present study on mass transport and its coupling with mechanical behaviour.

2. Experimental procedure and data analysis

For experimental validation of the model, cheese blocks were taken from the plant at the end of the brining step and ripened in the lab at two successive controlled temperatures: 12 °C (for 8–10 days) and 20 °C (for 15 days). Temperature was maintained constant using maturing cabinets (Grand Cru, Liebherr, France). For all the followings, the initial time $d = 0$ refers to the time at which the temperature of the ripening rooms was changed from 12 °C to 20 °C.

At each time chosen in the ripening process (when changing ripening temperature, and then at day 4, 5, 7, 8, 11, 12 and 15, depending on the experimental runs), one cheese block was taken out of the maturing cabinet and images were acquired, either by X-ray or MRI imaging (Table 1), on the whole cheese block, following the method developed by Musse, Challos, Huc, Quellec, and Mariette (2014). For each experimental campaign, the time-course changes in bubble volume were averaged in two separate regions of interest (ROI) that are under the rind and at core of the cheese blocks. The dimensions of these regions were 16 × 16 × 1.5 cm, the first one being located 1 cm under the rind and the second 4 cm. Since the position of the rind evolves with the inflation of bubbles during ripening, the location of these regions changed with respect to the fixed referential. Bubbles were considered to be in a given ROI if their barycentre belonged to it. Bubbles that had volumes lower than 10 mm³ and presented no growth during ripening were omitted. Standard deviation was of great magnitude (ranging from 8 to 150% over all the ripening), representative of the high variability in bubble size and growth kinetics within the cheese block. More details about the image analysis can be found in Huc, Mariette, et al., 2014.

Experimental conditions are summarised in Table 1.

Table 1
Experimental configurations.

	Run 1	Run 2	Run 3
Imaging technique	X-Ray	MRI	MRI
Replications	3	3	1
Days in cold room	10	8	8
Days in warm room	15	15	15

3. Model description

Except when stated, values are given at 20 °C and 101,325 Pa.

3.1. Geometry

In order to minimise computational cost, modelling was restricted to a single, spherical bubble surrounded by a spherical volume of cheese (representative volume of cheese around one bubble).

3.2. Hypotheses

Cheese was considered nearly-incompressible, with a Poisson ratio ν of 0.49. Its composition (other than CO₂), mechanical and diffusive properties were considered homogeneous at the scale considered. Carbon dioxide was also considered to be produced homogeneously. Within the bubble, pressure was considered uniform and gases other than carbon dioxide were neglected. Temperature was considered uniform and constant.

3.3. Mechanical behaviour

The behaviour of the cheese was modelled with a 5-element generalised Maxwell model described earlier in a dedicated paper (Laridon, Doursat, Grenier, Michon, Flick, & Lucas, 2015). The mechanical equilibrium was expressed through the conservation of momentum:

$$\nabla \cdot \sigma = \rho g \quad (1)$$

where σ is the stress, ρ the density and g the gravitational acceleration. Stress was calculated as the sum of elastic and viscoelastic parts and the viscoelastic part was described by the Maxwell model.

3.4. Mass transport

Mass diffusion was described according to Fick's law; mass conservation writes as follows:

$$\frac{\partial c}{\partial t} - D_{CO_2}^{ch} \Delta c = r_{CO_2} \quad (2)$$

where c is the number of moles of carbon dioxide in the water and fat phase of cheese by cubic meter of cheese, later denoted as the apparent carbon dioxide concentration in the domain, $D_{CO_2}^{ch}$ the apparent diffusivity of carbon dioxide in cheese (Section 4.2) and r_{CO_2} the carbon dioxide production rate within the cheese domain (Section 4.1). Carbon dioxide mass transport properties (solubility and diffusion) were considered of the same order of magnitude in the fat phase and water phase (Jakobsen et al., 2009).

The equilibrium at the gas-cheese interface was expressed according to Henry's law:

$$c_i = k_H^{ch} p_i \quad (3)$$

where c_i is the apparent carbon dioxide concentration at the interface, p_i the pressure exerted by the gas on the interface and k_H^{ch} , Henry's constant for carbon dioxide in cheese.

The atmospheric pressure p_{atm} is used as the pressure of reference in the mechanical aspects.

3.5. Coupling of transport phenomena

The carbon dioxide flux at the gas-cheese interface j_i can be written as:

$$j_i = -D_{CO_2}^{ch} \nabla c_i \cdot \mathbf{n} \quad (4)$$

where \mathbf{n} is the normal vector of the interface. This flux was numerically computed as:

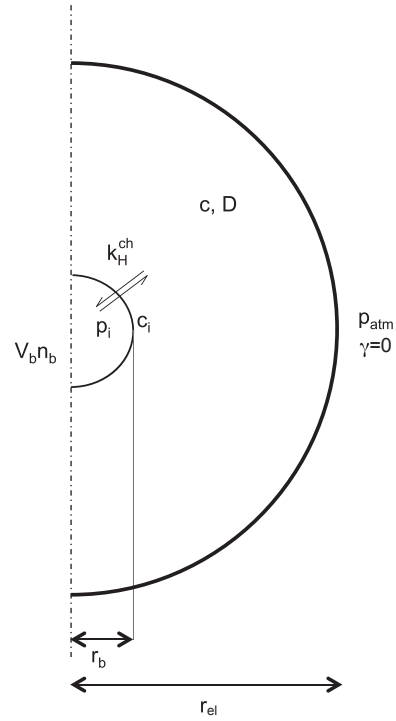


Fig. 1. Geometry used for modelling.

$$j_i = -\gamma (c_i - k_H^{ch} p_i) \quad (5)$$

where γ is the transfer coefficient at the interface. To ensure that the effect of diffusion in the cheese was limiting, the Biot number for mass transport was set at a high value (10^5):

$$Bi_m = \frac{\gamma L}{D_{CO_2}^{ch}} \quad (6)$$

This implied that γ was set at a high value and assured conditions very close to equilibrium ($\gamma \rightarrow \infty$ leads to Eq. (3)). Characteristic length L was set at 10 mm, as it was the typical length between the gas-cheese interface and the boundaries of the domain (Fig. 1).

Time-course change in the quantity of CO₂ in the gaseous phase, $\frac{dn_b}{dt}$, was deduced from the CO₂ flux:

$$\frac{dn_b}{dt} = \int_{\Gamma_i} j_i dS_i \quad (7)$$

where Γ_i is the gas-cheese interface boundary and S_i its surface.

Using Eqns. (5) and (7), and the ideal gas law, the following ODE was solved at the gas-cheese interface:

$$\frac{dn_b}{dt} = -\gamma \int_{\Gamma_i} c_i dS_i - \gamma k_H^{ch} RT \frac{S_i}{V_b} n_b \quad (8)$$

where V_b is the volume of the gaseous phase (bubble). The quantity of CO₂ determined with Eq. (8) was used to calculate the pressure of the gas at the gas-cheese interface with the cheese domain, following the ideal gas law:

$$p_i = \frac{n_b RT}{V_b} \quad (9)$$

The pressure calculated using Eq. (9) was used as mechanical boundary condition at the gas-cheese interface (Eq. (10)), and therefore constitutes the coupling between mechanical behaviour and mass transport.

3.6. Boundary conditions

3.6.1. Mechanical boundary conditions

Pressure calculated using Eq. (9) was applied at the bubble-cheese interface:

$$\sigma_i \cdot \mathbf{n} = -(p_i - P_{atm}) \quad (10)$$

where σ_i is the stress applied to the gas-cheese interface.

The other boundary was left free of stress.

3.6.2. Mass transfer boundary conditions

There was no flux of CO₂ at the outer boundary of the cheese sphere, except at the interface with the bubble, where the flux calculated by Eq. (5) was used.

Under these conditions, the growth of a bubble is considered with no mechanical constraint other than that exerted by the cheese material itself (restricted at the boundaries of the cheese sphere which contains a representative volume of cheese around on bubble). Mechanical interactions between adjacent bubbles were not reproduced. All the CO₂ produced in the cheese domain diffuses toward the bubble; competition for CO₂ between adjacent bubbles, or large-scale diffusion between regions of low and high CO₂ content at the cheese block scale were not taken into account.

3.7. Initial conditions

It is considered that at a time denoted by t_{sat} the cheese is saturated in CO₂. All the simulations began at this saturation time, with t defined as $t = t(days) - t_{sat}$. The initial bubble radius r_b in the simulation (2.17 mm) was set at the average experimental value observed at that time. The volume of cheese surrounding the bubble was also determined in average at that time ($4.2 \pm 2.0 \text{ cm}^3$).

3.7.1. Mechanical initial conditions

Equilibrium at the atmospheric pressure was considered,

$$p_i(t = 0) = P_{atm} \quad (11)$$

3.7.2. Mass transfer initial conditions

Following the initial saturation hypothesis, initial carbon dioxide concentration within the domain was defined as:

$$c(t = 0) = k_H^{\text{ch}} P_{atm} \quad (12)$$

The initial CO₂ quantity in the bubble was calculated with the help of ideal gas law:

$$n_b(t = 0) = \frac{P_{atm} V_b(t = 0)}{RT} \quad (13)$$

3.8. Numerical implementation and calculation

The model was implemented in COMSOL Multiphysics (COMSOL AB, Sweden). Simulations were conducted from the time at which saturation in CO₂ is reached to the end of warm room ripening (15 days).

4. Estimation of values for input parameters

4.1. Carbon dioxide production rate

Carbon dioxide production rates, r_{CO_2} , were measured on the same type of cheese as that used in the experiment, both at core and under rind (same locations as mentioned in Section 2 for the analysis of bubble volume). Cheese blocks used for these measurements were from different batches than those studied according to the protocol defined in Section 2 (data for validation of the model); different batches were used to characterise the inter-batch variability.

For each batch, about 20 cheese discs (2 mm thick at most) were deposited in a sealed bottle onto small grids of large mesh and separated from the other discs by a sustaining stand. The full device is detailed in Huc, Michon, et al. (2014).

The bottles were initially filled with N₂ at atmospheric pressure, and placed in a temperature-controlled environment at 20 °C. Nitrogen recreated the anaerobic conditions of bacterial growth during cheese ripening and also avoid the growth of moulds.

The pressure of the gas within the bottle, $p(t)$, was monitored over duration relevant of the ripening process (warm room). The time-course changes in pressure were attributed to the production of carbon dioxide only. Measurements were assumed to be diffusion-independent, because of the very low thickness of the cheese discs. The number of moles of CO₂ produced at a given time per volume of cheese was deduced from the pressure, using the ideal gas law:

$$\text{Produced } CO_2 = \frac{\rho^{\text{ch}} (p(t) - P_{atm}) V^{\text{gas}}}{m^{\text{ch}} RT} \quad (14)$$

where m^{ch} is the total mass of cheese discs in a bottle (about 25 g), measured before each experiment, and, V^{gas} , the gaseous volume surrounding the cheese discs in the bottle. The latter was estimated by subtracting the volume occupied by the cheese discs and the sustaining stand to the overall bottle volume. The volume of the bottle containing the sustaining stand was determined by filling the bottle with water and calculating the volume by weighing the water.

The amount of CO₂ produced during the experiment relative to the

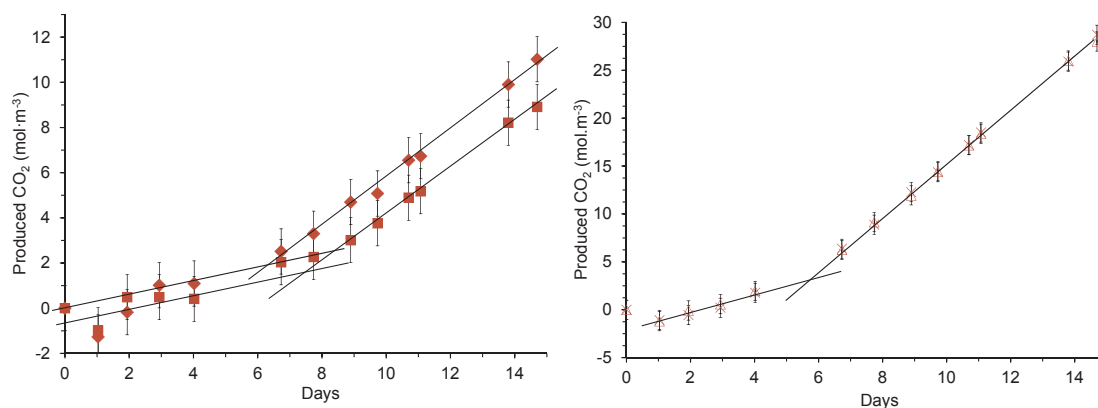


Fig. 2. Carbon dioxide production under rind (left) and at core (right) at 20 °C. Two replications are shown for each graph, i.e. one bottle associated to one cheese block. Note that the scale of the y-axis differs between the two Figures (production of CO₂ in cheese samples under rind was decreased by 1/3 at least compared to the core).

Table 2

Rate of CO₂ production in cheese (mol·m⁻³·s⁻¹); standard deviations were calculated on 5 and 7 experimental curves for Stage I and Stage II (respectively), with two replicates each, and were attributed to the intra- and inter-batch variability.

mol·m ⁻³ ·s ⁻¹	Stage I		Stage II		Ratio between stages I and II
	Mean	st. dev.	Mean	st. dev.	
At core	1.65·10 ⁻⁵	29%	3.56·10 ⁻⁵	23%	2.2
Under rind	5.02·10 ⁻⁶	31%	1.37·10 ⁻⁵	11%	2.7

cheese volume is presented in Fig. 2.

At the very beginning of the experiment (until one day at most), a slight decrease in pressure could be observed and was attributed to the entrance of nitrogen into the cheese.

The carbon dioxide production rate was not constant over time. Production rates were calculated by linear regression of experimental data obtained between days 2 and 4 for the first stage, and between days 7 and 14 for the second stage. Mean values reported in Table 2 were calculated on 5–7 experimental runs, 2 replicates each. Hence the associated standard error was relevant to intra- and inter-batch variability. The time at which the break point between stages I and II was observed, t_r , was equal to 5.5 ± 1.9 days, taking into account both under rind and core data.

At the beginning of warm room (until 6 days in Fig. 2) the production rate was 2 times lower than afterwards, both at core and under rind (Table 2). The effect of several factors onto the rate of production was investigated experimentally in the literature, among them the impact of salt content, and moisture content. Cheeses without salt yielded production rates that were up to 2.6 times as much as standard industrial cheeses (Huc, Michon, et al., 2014), whereas for the two moisture contents considered (42 and 46%), there was no impact on the production rate. However, for cheeses that had the highest moisture content, production of carbon dioxide occurred 3 days after the change of room temperature.

4.2. Carbon dioxide diffusivity

Diffusivity of carbon dioxide in cheese $D_{CO_2}^{ch}$ was calculated from carbon dioxide diffusivity in water $D_{CO_2}^w$ (Davidson & Cullen, 1957); the same value was applied to the liquid fat phase. Diffusivity of CO₂ in water was then weighted by the volume fraction of water in cheese X^w and the volume fraction of non-crystallised fat X^{fat} , and the tortuosity of the cheese material \mathcal{F} :

$$D_{CO_2}^{ch} = (X^w + X^{fat}) \frac{D_{CO_2}^w}{\mathcal{F}} \quad (15)$$

Tortuosity was assumed to be at $\pi/2$ due to the presence of protein and fat globules. X^w was set at 0.42, considering that all the water present in the cheese material is available for CO₂ diffusion, and X^{fat} was set at 0.15, considering that only 55% of the fat phase was not crystallised. This yielded $D_{CO_2}^{ch} = 6.09 \cdot 10^{-10} \text{ m}^2 \text{ s}^{-1}$, compared to $1.68 \cdot 10^{-9} \text{ m}^2 \text{ s}^{-1}$ for $D_{CO_2}^w$. It should be noted that this assessment method is consistent with the order of magnitude of the values provided by Acerbi, Guillard, Guillaume, Saubanere, et al. (2016) on similar cheeses, ranging between 1 and $9 \cdot 10^{-10} \text{ m}^2 \text{ s}^{-1}$, depending on the factor studied (salt and moisture content, age, PTA/TN).

4.3. Carbon dioxide concentration in cheese and saturation

The values below were considered in cheese material and in pure water.

CO₂ concentration at saturation can be estimated from Henry's constant value reported in the literature. Temperature dependency of k_H^w is given by:

$$k_H^w = k_H^w(T_{std}) \exp\left(-\frac{\Delta H}{R} \left(\frac{1}{T} - \frac{1}{T_{std}}\right)\right) \quad (16)$$

where $T_{std} = 25 \text{ }^\circ\text{C}$, T is the temperature of the warm room in the ripening process ($20 \text{ }^\circ\text{C}$), and ΔH the standard enthalpy set at $1.995 \cdot 10^{-4} \text{ J}\cdot\text{mol}^{-1}$ (Sander, 2014), R is the ideal gas constant ($8.314 \text{ J}\cdot\text{mol}^{-1}\cdot\text{K}^{-1}$).

Henry's constant equivalent for the cheese considered can be determined from the Henry's constant for CO₂ in pure water, using Eq. (18):

$$k_H^{ch} = (X^w + X^{fat}) k_H^w \quad (17)$$

Total pressure within the bubbles is of the same order of magnitude than the atmospheric pressure, with a slight overpressure (about 2%, Grenier, Laridon, Le Ray, Challos, & Lucas, 2016), and the bubbles contain mainly carbon dioxide. CO₂ concentration at saturation in pure water s^w under the same conditions is given by:

$$s^w = P_{atm} k_H^w \quad (18)$$

where k_H^w is Henry's constant value. This yielded a value of 29.7 mol of CO₂ per m³ of pure water at $20 \text{ }^\circ\text{C}$, which is in accord with the order of magnitude of experimental results obtained on similar cheese by Acerbi, Guillard, Guillaume, and Gontard (2016).

CO₂ concentration expected at saturation in the water and fat phase in cheese s^{ch} was found to be equal to 16.87 mol of CO₂ per m³ of cheese at core, and 16.29 under rind.

CO₂ concentration values were assessed experimentally on the same type of cheese used in this study, following a method similar to that used in Jakobsen et al. (2009). These measurements showed that, when entering the warm room, CO₂ concentration exceeded or was very close to this theoretical saturation value. Concentration reached a value of 20.6 ± 1.5 and 16.1 ± 1.5 mol of CO₂ per m³ of cheese at core and under the rind, respectively. However, simulations were still maintained with an initial CO₂ concentration in the domain at the theoretical saturation value in order to ensure mass equilibrium between the gas and liquid phases at the start of the simulations.

4.4. Mechanical properties of cheese

Values of the parameters of the Maxwell model were fixed according to the average values that were determined on the same type of semi-cheese than the one under study (Table 2). See Laridon et al. (2016) for further details about the mechanical test and the data analysis.

5. Results and discussion

5.1. Simulation with reference values of input parameters at the core of the cheese block

Fig. 3 presents the growth of a single bubble simulated with the numerical model using reference values of input parameters characteristic of the core of the cheese block (Table 3); the simulated data are also compared to the experimental one from three runs, averaging the behaviour of about 10 bubbles each, located at the cheese block core. The simulation agreed with the experiment, in a qualitative manner. Despite the attention given to the estimation of input parameters, there was discrepancy between simulation and experiment at short ripening times.

Hence, a sensitivity study was performed in order to characterise the relative influence of the model inputs on the outputs i.e. the bubble volume.

5.2. Sensitivity study of the model to input parameters characterised at core

The primary objective of the sensitivity study was to evaluate which input parameter was more prone to adjustment for better fitting of the

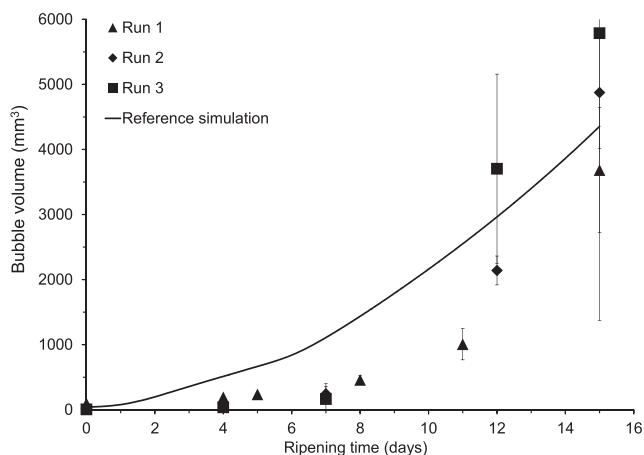


Fig. 3. Experimental averaged and simulated bubble volume at core. Runs involved a cheese block coming from a different batch, each being separated by several months.

experimental trend, and the secondary objective was to highlight the parameters that could be modified in the conduction of the process for enhancing bubble growth for instance. Table 3 summarises the upper and lower values around the reference value for each input parameter in this sensitivity study. Each parameter was varied separately, all other parameters being kept at their reference values.

For the mechanical aspects, only the relaxation properties of the last Maxwell element were varied, as they proved to be the most influential parameters on bubble growth (Y. Laridon et al., 2016); their variations around the reference value (Table 3) corresponded to the inter-batch variability ($\pm \sigma$). A $\pm 75\%$ sweep was used for the diffusivity of CO₂ within the cheese, allowing covering the range of variation reported for this type of measurements in Acerbi, Guillard, Guillaume, Saubanere, et al. (2016). Production rate was swept according to the inter-batch variability estimated in Section 4.1, taking into account the highest standard deviation obtained between stages I and II. The volume of cheese surrounding the bubble was also swept in order to take into account both intra- and inter-batch variability. For further discussion of the results, an additional simulation was run with a non-limiting value (20 cm³).

The variations of initial bubble volumes were representative of extreme behaviour encountered in the experiments.

In order to rank the most influential parameters on bubble growth, sensitivity indices I_k were calculated for each input parameter X_k as:

$$I_k = 100 \frac{\left| \frac{V_b(X_k^{max}) - V_b(X_k^{ref})}{V_b(X_k^{ref})} \right| + \left| \frac{V_b(X_k^{min}) - V_b(X_k^{ref})}{V_b(X_k^{ref})} \right|}{\left| \frac{X_k^{max} - X_k^{ref}}{X_k^{ref}} \right| + \left| \frac{X_k^{min} - X_k^{ref}}{X_k^{ref}} \right|} \quad (19)$$

The sensitivity indices were assessed at the end of the simulations (15 days) and reported in Table 3. Simulated growth of bubbles obtained with the numerical model using some of these values of input parameters were also compared to the experimental data (Fig. 4).

The mechanical parameters of the 5th Maxwell element proved to be the least influential parameters over bubble growth, having sensitivity indices at least 60 times lower than the most influential parameter (Table 3). Values of mechanical parameters typically encountered under rind did not even oppose much more resistance to the bubble growth (data not reported). Initial bubble volume proved to have little influence over the bubble growth (Table 3) though it must be noted that the smallest bubbles benefited from a higher surface-to-volume ratio, and subsequently yielded higher volumes at the end of ripening. Henry's constant had also a small impact, confirming that the rough estimate taken from the literature for this study did suffice.

Besides the cheese volume surrounding the bubble, parameters related to the mass transport or production showed the greatest influence on the bubble volume.

Simulated results were consistent with the experimental data, with an overestimation at short ripening times (Fig. 3). However, this overestimation could be also balanced if considering lower cheese volume available around the bubble (Fig. 4a), lower production rate (Fig. 4b) or lower diffusivity (Fig. 4c).

The carbon dioxide production rate in cheese proved to be nearly as important for the bubble growth as the cheese volume (Table 3). High sensitivity of bubble growth to carbon dioxide production, combined to the high inter-batches variability of this parameter (about 30%), argued in favour of measuring it specifically on a cheese block from the same batch, if accurate validation of the model is required.

Carbon dioxide diffusivity in cheese was the only parameter that was not specifically determined on the cheese material under study but was deduced from the diffusivity in pure water (Section 4.2). Simulated bubble volume obtained with the lower value of diffusivity proved to reproduce results that were a better fit to experimental data, especially at the beginning of the ripening (Fig. 4c). Lower diffusivity than expected can be explained by the fact that all the water is not available for the carbon dioxide to diffuse or that the tortuosity of the material has been underestimated. Indeed, tortuosity was set at $\pi/2$ under the hypothesis that fat and protein were spherical, but because of the cheese structure complexity, the tortuosity value may be higher. This result,

Table 3

Values of input parameters and the associated sensitivity indices of the bubble volume to each variation of each input parameter for the screening study including the reference set of values. I_k was determined on day 15.

	Reference	Lower value	Upper value	Variation (%)	I_k
λ_5 (s)	9324	6428	12,230	± 31	0.6
α_5	0.04	0.03	0.05	± 25	2.5
$D_{CO_2}^{ch}$ ($10^{-10} \text{ m}^2 \text{ s}^{-1}$)	6.1	1.5	10.7	± 75	26
r_{CO_2} ($\text{mol}\cdot\text{m}^{-3}\cdot\text{s}^{-1}$)	Stage I	$1.65\cdot 10^{-5}$	$2.13\cdot 10^{-5}$	± 29	111
	Stage II	$3.56\cdot 10^{-5}$	$4.37\cdot 10^{-5}$	± 23	
k_H^{ch} ($\text{mol}\cdot\text{m}^{-3}\cdot\text{Pa}^{-1}$)	$1.67\cdot 10^{-4}$	$1.25\cdot 10^{-4}$	$2.08\cdot 10^{-4}$	± 25	0.3
$V_b(t=0)$ (10^{-9} m^3)	42.6	5.4	96	$-87 + 125$	4.2
V^{ch} (10^{-6} m^3)	4.2	2.2	6.2	± 47	156

λ_5 and α_5 : mechanical parameters for the longest relaxation time (see Laridon et al., 2015).

$D_{CO_2}^{ch}$: carbon dioxide diffusivity in the cheese.

r_{CO_2} : carbon dioxide production rate.

k_H^{ch} : solubility of carbon dioxide in cheese.

V_b : bubble volume.

V^{ch} : cheese volume surrounding the bubble.

I_k : sensitivity index (see Section 5.2).

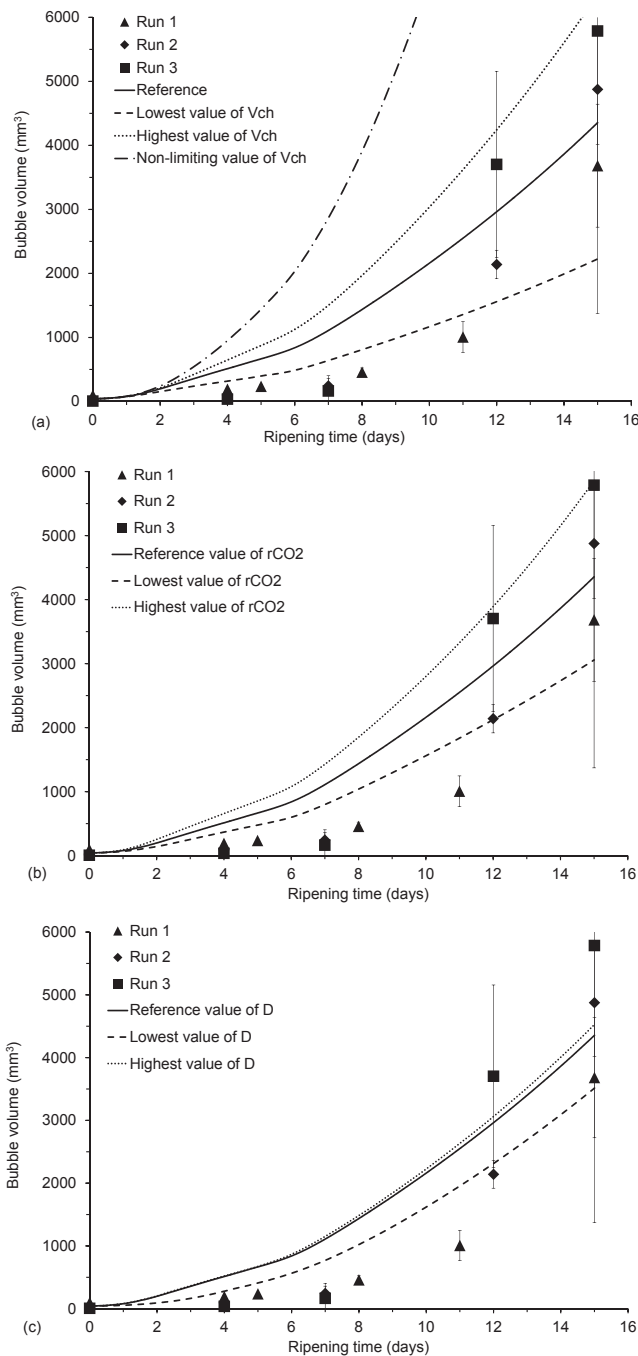


Fig. 4. Experimental and simulated bubble volumes at the core of the cheese block. Effect of the variations of input parameters of the model, (a) V^{ch} , (b) r_{CO_2} , (c) $D_{CO_2}^{ch}$, all other parameters being set at fixed value. Runs involved a cheese block coming from a different batch, each being separated by several months.

together with the high-ranking value of this input parameter in the sensitivity study also encourages further effort for experimental characterisation of carbon dioxide diffusivity in cheese. Let us remind from the introduction section that there is only one paper providing such data in the literature (Acerbi, Guillard, Guillaume, Saubanere, et al., 2016).

In the experiment, the initial rate of bubble growth was low despite of CO_2 saturation (Fig. 4) and low levels of diffusivity were assumingly incriminated (Huc, Michon, et al., 2014). Results from the present study also showed a contribution of the lower CO_2 production for ripening times lower than 5–6 days (Fig. 2).

The relatively small effect of $D_{CO_2}^{ch}$ on bubble growth (nearly 6 times

lower than the most influential parameter) was well illustrated in Fig. 4c, despite the wide variations of this input parameter. The system behaved as if the amount of CO_2 produced in cheese was limiting, which was consistent with the great effect of the increase in cheese volume surrounding the bubble (Fig. 4a).

Suppl. Mat. 1 gives the evolution of the screening index over the simulation time and allows to comprehend the evolution of the influence of each parameter over time.

5.3. Considerations about the spatial variability of the model parameters

For this study, two regions of interest (ROI) were considered in the cheese block: at core and under the rind. The two ROI considered experimentally were 3 cm from each other. Assuming diffusivity of CO_2 of the order of $10^{-10} m^2 s^{-1}$, this yielded a characteristic diffusion time of about 100 days between these two regions, which was significantly higher than the average stay in warm room (about 15 days). Therefore, the two ROI could be considered independently from each other, from a mass transport point of view.

In order to further validate the model, simulations were conducted for parameter values specific of the cheese region under the rind. In particular, production of CO_2 was set at its value measured for cheese material sampled under rind (Table 2), and the other parameters were set in accordance with the lower X^w and X^{fat} values found under the rind, typically at 0.40 and 0.15, respectively. At last, the cheese volume surrounding the bubble was set at $7.6 cm^3$ (average experimental value). Following the results at core, the diffusivity was set at its lowest value.

Compared to the simulations at core, simulations under the rind yielded better agreement in the first half of the ripening time. However, the simulated bubble volume was too high for the second half of the ripening time, at nearly twice the experimental value at the end (Reference curve in Fig. 5). Similarly to the results at core (Section 5.2), two simulations were conducted by varying V^{ch} and r_{CO_2} to cover the intra- and inter-batch variability. While the highest values (representing the most favourable conditions for bubble growth) yielded poor agreement with experiment, the least favourable condition (lowest V^{ch} and r_{CO_2}) yielded good agreement with experiment. This adds up to the conclusions made previously about the need of measurement of these properties for this specific food material.

Another explanation might come from the fact that it was assumed saturation in CO_2 under the rind was reached at the beginning of the warm room. Inter-batch variability of this parameter was not characterised under rind, and a lower carbon dioxide concentration when entering the warm room would mean that the simulations would have

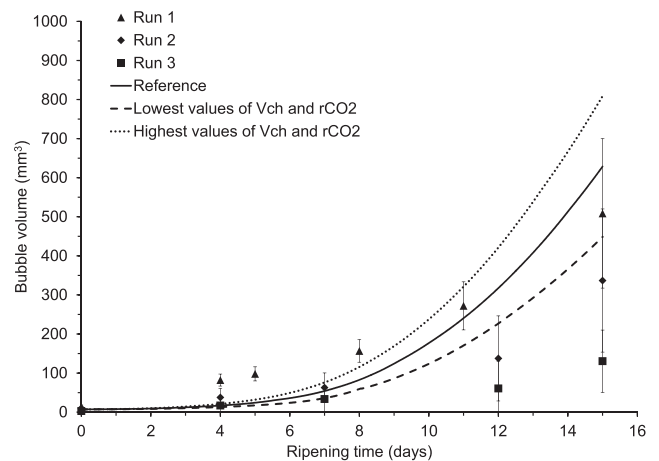


Fig. 5. Experimental and simulated bubble volumes under the rind. Runs involved a cheese block coming from a different batch, each being separated by several months.

to be started whenever the actual saturation was reached. Given that the production rates are lower under rind (Table 2) and depending on the actual carbon dioxide concentration at $d = 0$, a better fit could be achieved.

6. Conclusions

The growth of bubbles in cheese was investigated both experimentally and by simulation. Bubble volumes in cheese blocks during ripening were assessed experimentally with the help of X-Ray imaging and MRI with a dedicated image processing method. Special care was taken on the determination of the model parameters. One third of the input parameters were assessed from the literature. The other two thirds were assessed from dedicated measurements performed on the cheese material under study. A sensitivity study was conducted on the bubble growth model in order to rank the input parameters that were the most influential and brought some teachings for improving their estimate.

The model proved to reproduce the average bubble growth in cheese in a qualitative manner. This was yet a satisfactory result, keeping in mind that not all phenomena taking place at the cheese block scale (the scale of experimental data used for validation) were taken into account with such a simplistic model, relevant of the bubble scale.

Production of carbon dioxide, r_{CO_2} , and cheese volume surrounding the bubble, V^{ch} , were the most influential input parameters on the bubble growth. The experimental data also showed to be quite variable between batches, with a standard deviation ranging from 30% for the production rate to 50% for the cheese volume. This conclusion argued in favour of high number of repetitions (for instance more than three runs retained for the monitoring of bubble growth) in order to attain a more complete validation of the model. The only input parameter that was not determined experimentally and that revealed of high influence on bubble growth, $D_{CO_2}^{ch}$, was adjusted to fit the experimental sets of data with better agreement. Lower diffusivity of carbon dioxide than expected was explained by either an underestimation of tortuosity (initially assumed for spherically-shaped and regularly arranged obstacles) or an overestimation of the space available for diffusion (it was assumed for the first-hand estimation of diffusivity that the whole fraction of water was available for carbon dioxide diffusion). This highlighted the need of the measurement of this property in cheese, still lacking in the literature.

Finally, the mechanical behaviour of cheese or initial bubble volume proved not to have any effect on bubble growth.

CRedit authorship contribution statement

Y. Laridon: Conceptualization, Methodology, Software, Validation, Formal analysis, Investigation, Data curation, Writing - original draft, Writing - review & editing, Visualization. **D. Grenier:** Validation, Data curation, Writing - review & editing, Supervision. **C. Doursat:** Conceptualization, Software. **D. Huc:** Investigation, Data curation. **N. Roland:** Investigation, Data curation. **D. Flick:** Conceptualization, Methodology, Validation, Supervision. **T. Lucas:** Conceptualization, Methodology, Validation, Writing - review & editing, Supervision.

Declaration of Competing Interest

The authors declared that there is no conflict of interest.

Acknowledgements

This study was carried out with financial support from VALORIAL and the Regional Councils of Bretagne, Pays de Loire and Basse-Normandie. The first author, Yannick Laridon, is the holder of a grant from INRA and Irstea.

Appendix A. Supplementary material

Supplementary data to this article can be found online at <https://doi.org/10.1016/j.foodres.2019.108858>.

References

- Acerbi, F., Guillard, V., Guillaume, C., & Gontard, N. (2016). Impact of selected composition and ripening conditions on CO₂ solubility in semi-hard cheese. *Food Chemistry*, 192, 805–812. <https://doi.org/10.1016/j.foodchem.2015.07.049>.
- Acerbi, F., Guillard, V., Guillaume, C., Saubane, M., & Gontard, N. (2016). An appraisal of the impact of compositional and ripening parameters on CO₂ diffusivity in semi-hard cheese. *Food Chemistry*, 194, 1172–1179. <https://doi.org/10.1016/j.foodchem.2015.08.020>.
- Akkerman, J. C., Walstra, P., & Dijk, van H. J. M. (1989). Holes in Dutch type cheese. 1. Conditions allowing eye formation. *Netherlands Milk and Dairy Journal* <https://doi.org/urn:nbn:nl:ui:32-10315>.
- Amon, M., & Denson, C. D. (1984). A study of the dynamics of foam growth: Analysis of the growth of closely spaced spherical bubbles. *Polymer Engineering & Science*, 24(13), 1026–1034. <https://doi.org/10.1002/pen.760241306>.
- Bisperink, C. G. J., & Prins, A. (1994). Bubble growth in carbonated liquids. *Colloids and Surfaces A: Physicochemical and Engineering Aspects*, 85(2–3), 237–253 [https://doi.org/10.1016/0927-7757\(94\)00088-X](https://doi.org/10.1016/0927-7757(94)00088-X).
- Blanc, B., Bossert, J. O., Martin, B., & Jimeno, J. (1983). Gas exchanges at the surface of Gruyere cheese during ripening. *Schweizerische Milchwirtschaftliche Forschung*, 12, 30–34.
- Campbell, G. M., & Mougeot, E. (1999). Creation and characterisation of aerated food products. *Trends in Food Science & Technology*, 10(9), 283–296. [https://doi.org/10.1016/S0924-2244\(00\)00008-X](https://doi.org/10.1016/S0924-2244(00)00008-X).
- Davidson, J. F., & Cullen, M. A. (1957). The determination of diffusion coefficients for sparingly soluble gases in liquids. *Transactions of the Institution of Chemical Engineers*, 35, 51–60.
- De Cindio, B., & Corraera, S. (1995). Mathematical modelling of leavened cereal goods. *Journal of Food Engineering*, 24(3), 379–403. [https://doi.org/10.1016/0260-8774\(95\)90052-D](https://doi.org/10.1016/0260-8774(95)90052-D).
- Fan, J. T., Mitchell, J. R., & Blanshard, J. M. V. (1999). A model for the oven rise of dough during baking. *Journal of Food Engineering*, 41(2), 69–77. [https://doi.org/10.1016/S0260-8774\(99\)00070-9](https://doi.org/10.1016/S0260-8774(99)00070-9).
- Grenier, D., Laridon, Y., Le Ray, D., Challos, S., & Lucas, T. (2016). Monitoring of single eye growth under known gas pressure: Magnetic resonance imaging measurements and insights into the mechanical behaviour of a semi-hard cheese. *Journal of Food Engineering*, 171, 119–128. <https://doi.org/10.1016/j.jfoodeng.2015.10.018>.
- Guggisberg, D., Schuetz, P., Winkler, H., Amrein, R., Jakob, E., Fröhlich-Wyder, M.-T., ... Wechsler, D. (2015). Mechanism and control of the eye formation in cheese. *International Dairy Journal*, 47, 118–127. <https://doi.org/10.1016/j.idairyj.2015.03.001>.
- Hailemariam, L., Okos, M., & Campanella, O. (2007). A mathematical model for the isothermal growth of bubbles in wheat dough. *Journal of Food Engineering*, 82(4), 466–477. <https://doi.org/10.1016/j.jfoodeng.2007.03.006>.
- Huc, D., Mariette, F., Challos, S., Barreau, J., & Moulin, G. (2014). Multi-scale investigation of eyes in semi-hard cheese. *Innovative Food Science and Emerging Technologies*. <https://doi.org/10.1016/j.ifset.2013.10.002>.
- Huc, D., Michon, C., Roland, N., Challos, S., & Mariette, F. (2014). Study of the influence of salt content on eye growth in semi-hard cheeses using MRI and CO₂ production measurements. *International Dairy Journal*. <https://doi.org/10.1016/j.idairyj.2013.11.010>.
- ITFF-ITG/Actilait (1984). Production de gaz carbonique et formation de l'ouverture dans l'emmental et le Comté. Etude ITG SS 1984/05/C. Technical report.
- Jakobsen, M., Jensen, P. N., & Risbo, J. (2009). Assessment of carbon dioxide solubility coefficients for semihard cheeses: The effect of temperature and fat content. *European Food Research and Technology*, 229, 287–294. <https://doi.org/10.1007/s00217-009-1059-3>.
- Jones, S. F., Evans, G. M., & Galvin, K. P. (1999). Bubble nucleation from gas cavities – A review. *Advances in Colloid and Interface Science*, 80, 27–50. [https://doi.org/10.1016/S0001-8686\(98\)00074-8](https://doi.org/10.1016/S0001-8686(98)00074-8).
- Keentok, M., Newberry, M. P., Gras, P., Bekes, F., & Tanner, R. I. (2002). The rheology of bread dough made from four commercial flours. *Rheologica Acta*, 41, 173–179. <https://doi.org/10.1007/s003970200016>.
- Laridon, Y., Doursat, C., Grenier, D., Michon, C., Flick, D., & Lucas, T. (2015). Identification of broad-spectrum viscoelastic parameters: Influence of experimental bias on their accuracy and application to semihard-type cheese. *Journal of Rheology* (1978-present), 59(4), 1019–1044. <https://doi.org/10.1122/1.4922221>.
- Laridon, Y., Grenier, D., Houeix, D., Doursat, C., Lucas, T., & Flick, D. (2016). Modelling of the growth of a single bubble in semi-hard cheese, with experimental verification and sensitivity analysis. *Applied Mathematical Modelling*, 40, 10771–10782. <https://doi.org/10.1016/j.apm.2016.08.018>.
- Launay, B., & Michon, C. (2008). Biaxial extension of wheat flour doughs: Lubricated squeezing flow and stress relaxation properties. *Journal of Texture Studies*, 39, 496–529. <https://doi.org/10.1111/j.1745-4603.2008.00156.x>.
- Liger-Belair, G., Parmentier, M., & Jeandet, P. (2006). Modeling the kinetics of bubble nucleation in champagne and carbonated beverages. *The Journal of Physical Chemistry B*, 110(42), 21145–21151 <https://doi.org/10.1021/jz044222i>.
- Musse, M., Challos, S., Huc, D., Quellec, S., & Mariette, F. (2014). MRI method for investigation of eye growth in semi-hard cheese. *Journal of Food Engineering*, 121,

- 152–158. <https://doi.org/10.1016/j.jfoodeng.2013.08.010>.
- Rodríguez-Aguilera, R., Oliveira, J. C., Montanez, J. C., & Mahajan, P. V. (2009). Gas exchange dynamics in modified atmosphere packaging of soft cheese. *Journal of Food Engineering*, 95, 438–445. <https://doi.org/10.1016/j.jfoodeng.2009.06.021>.
- Sander, R. (2014). Compilation of Henry's law constants, version 3.99. *Atmospheric Chemistry and Physics Discussions*, 14(21), 29615–30521. <https://doi.org/10.5194/acpd-14-29615-2014>.
- Schuetz, P., Guggisberg, D., Jerjen, I., Fröhlich-Wyder, M. T., Hofmann, J., Wechsler, D., ... Bachmann, H. P. (2013). Quantitative comparison of the eye formation in cheese using radiography and computed tomography data. *International Dairy Journal*, 31, 150–155. <https://doi.org/10.1016/j.idairyj.2012.12.007>.
- Seuvre, A. M., & Mathlouthi, M. (1982). Contribution to the Study of Gas-Release during the Maturation of a French Emmental Cheese. *Lebensmittel-Wissenschaft & Technologie*, 15, 258–262.
- Shah, P., Campbell, G. M., McKee, S. L., & Rielly, C. D. (1998). *Proving of bread dough: Modelling the growth of individual bubbles*, Vol. 76. Institution of Chemical Engineers.
- Vivier, D., Compan, D., Moulin, G., & Galzy, P. (1996). Study of carbon dioxide release from Feta cheese. *Food Research International*, 29, 169–174. [https://doi.org/10.1016/0963-9969\(96\)00001-4](https://doi.org/10.1016/0963-9969(96)00001-4).